Second nonequilibrium-phonon bottleneck for carrier cooling in highly excited polar semiconductors

A. Žukauskas*
Institute of Materials Science and Applied Research, Vilnius University, Naugarduko 24, 2006 Vilnius, Lithuania
(Received 30 October 1997)

Cooling of high-density electron-hole plasma excited in direct-gap polar semiconductors by a picosecond pulse of an extreme intensity is considered. Convenient models of carrier coupling with LO phonons via screened Fröhlich interaction, nonequilibrium LO-phonon creation by free-carrier intraband relaxation, and fermion recombination-induced heating were combined with a description of second-generation nonequilibrium phonons produced by anharmonic decay of the nonequilibrium LO phonons. An additional source of nonequilibrium LO phonons due to nonradiative capture by deep centers via multiphonon emission was also introduced. A numerical simulation for a CdS crystal was performed. Even at room temperature, the carrier cooling is shown to exhibit a noticeable slow component for plasma densities above 10^{19} cm^{-3}. At the late stage of the relaxation, the relevant time constant ($\sim$100 ps) is found to be comparable with the carrier lifetime, while the magnitude of the excess effective temperature is determined by nonequilibrium population of the second-generation phonons. The ''width'' of the second nonequilibrium-phonon bottleneck is demonstrated to be determined by peculiarities of the lattice vibration spectrum. [S0163-1829(98)04423-3]

I. INTRODUCTION

In recent decades, cooling of quasithermalized electron-hole plasma in highly photoexcited semiconductors has been extensively investigated both for unveiling fundamental interactions in solid state and for modeling energy-transfer processes in devices. Summarization of the experimental data reveals a general tendency for slowing down the carrier mean-energy relaxation with increasing excitation density. The first observation of the effect[1] was attributed to screening of the carrier-phonon interaction. Subsequent experimental studies[2–4] have stimulated a development of the idea that the cooling rate may be reduced because of a buildup of nonequilibrium-optical-phonon population.[5] In Ref. 6, a detailed description of carrier cooling including nonequilibrium-optical-phonon reabsorption was presented and used for explanation of the experimental data. This concept is successfully applied up to nowadays[7–9] for carrier densities below 10^{19} cm^{-3}, which are usually produced in semiconductor objects by means of high-repetition-rate picosecond and femtosecond lasers. It should be noted that nonequilibrium optical phonons may result in an extremely slow (nanosecond-scaled) carrier cooling at low ambient temperatures ($k_BT_0 \ll \hbar\omega$, ω is the optical-phonon frequency), when the phonon quasitemperature[9] logarithmically depends on the average occupation number, which relaxes with time constants of the picosecond order.[10] This is not possible for high ambient temperatures, when the average occupation number is linearly related to the phonon quasitemperature. Nevertheless, a lot of experimental evidence obtained at room temperature under extremely high photoexcitation by means of low-repetition lasers[11–18] indicated an existence of a slow component in the cooling process that could not be attributed either to the screening (if properly treated) or to a trivial lattice heating. A simple model of long-lived second-generation (daughter) phonons, produced by anharmonic decay of the optical ones and hindering the relaxation through recurrent anharmonic fusion, was thus proposed[16,17] to account for the observed phenomenon. However, the room-temperature values of the daughter-phonon lifetimes required to be introduced in this model ($\sim$100 ps) (Refs. 19 and 20), were too large to be widely accepted. Furthermore, an improved treatment of nonequilibrium daughter phonons for a GaAs-type lattice dynamics[21,22] has shown that the fusion to the short-wavelength region of the optical branch makes the hindering process negligible. In spite of this, the question of the role of second-generation nonequilibrium phonons in carrier cooling is still open.[8,23,24] This problem may also emerge with further investigation of nonequilibrium phonons in ''heavy-duty'' semiconductors such as GaN,[25] which recently attracted much attention.

On the other hand, there exist mechanisms, maintaining the carrier and phonon temperatures above the equilibrium one throughout the whole carrier lifetime. One of them is recombination-induced heating of fermions[26,27] occurring due to mean-energy dependence on carrier density. Another possible one is generation of nonequilibrium optical phonons during carrier nonradiative capture via multiphonon emission (MPE). This recombination route dominates at elevated temperatures in crystals with strong electron-phonon coupling,[28] including the high-excitation regime.[29] At first sight, these recombination-heating mechanisms are expected to manifest themselves only at low ambient temperatures because of their relatively low efficiency.

In the present work, an attempt is made to treat the carrier cooling within a model incorporating most relevant energy-transfer routes in highly excited polar crystals (Sec. II). Low-efficiency carrier recombination heating (both due to intrinsic fermion effects[26] and due to capture by deep centers via MPE) is considered here in combination with nonequilibrium phonons of two generations. Then, in Sec. III, calculations of transient behavior of carrier effective temperature are performed, using reasonable values of the depopulation time constants, and factors, responsible for the occurrence of second nonequilibrium-phonon bottleneck in the carrier cooling, are discussed in detail. Conclusions are presented in Sec. IV.

 © 1998 The American Physical Society

II. THE MODEL

Consider plasma with the density of electron-hole pairs n, homogeneously photogenerated in a semiconductor specimen. The plasma may be of any degree of degeneracy with the relevant fermion effects taken into consideration. The density is assumed to be high enough to ensure a rapid scattering of just generated electrons and holes by intercarrier collisions and to establish Fermi-Dirac distribution functions for both carrier subsystems with a uniform effective temperature T,

$$f_i(E)=\left[\exp\left(\frac{E}{k_BT}-\eta_i\right)+1\right]^{-1}, \tag{1}$$

where $\eta_i=\xi_i/(k_BT)$, and ξ_i are the Fermi quasilevels for electrons ($i=e$) and holes ($i=h$). The electrons and holes are supposed to reside within the simple parabolic bands with spherical symmetry. We shall reduce our consideration to the case when the carriers interact predominantly with the only one dispersionless LO phonon branch. This is a fair high-temperature ($T\geqslant 50$ K) approximation for II-VI compound semiconductors such as CdS and CdSe with the dominant long-range Fröhlich carrier-phonon interaction, as well as a quite realistic approach for III-V crystals where, however, deformation-potential scattering of holes may be also significant. The nonequilibrium LO phonons produced by hot carriers are supposed to decay by a three-phonon anharmonic process into lower-energy phonons (daughter phonons) with the frequency around half of that of LO phonons (subharmonic frequency). We shall treat the daughter phonons as linearly dispersed, but the problem will not be reduced to the case of acoustic phonons.[21,22,30] This means that the daughter phonons generally may be optical as in CdS, CdSe, and other nonsphalerite crystals.

The main problem of the present consideration is to find out the transient behavior of the carrier effective temperature and to establish the factors governing the cooling time constant on the late stage of the relaxation after the excitation by a pulse of a picosecond duration. Following the sequence of Ref. 26, the rate of the effective temperature variation for fermion plasma can be formally derived from the differentiation of the carrier mean energy

$$\frac{d\langle E\rangle}{dt}=\frac{\partial\langle E\rangle}{\partial n}\frac{dn}{dt}+\frac{\partial\langle E\rangle}{\partial T}\frac{dT}{dt}. \tag{2}$$

The mean energy per unit volume with neglect of carrier interaction is

$$\langle E\rangle=\frac{3}{2}k_BTn\sum_{i=e,h}\frac{F_{3/2}(\eta_i)}{F_{1/2}(\eta_i)}=\frac{3}{2}k_BT\sum_i B^{3/2}_{1/2}(\eta_i), \tag{3}$$

where $F_j(\eta_i)$ is the Fermi integral of the order j. A notation $B^{\alpha}_{\beta}(\eta_i)=F_{\alpha}(\eta_i)/F_{\beta}(\eta_i)$ is introduced for convenience.

On the other hand, the rate of the mean-energy variation is

$$\frac{d\langle E\rangle}{dt}=\left(\frac{\partial\langle E\rangle}{\partial t}\right)_G+\left(\frac{\partial\langle E\rangle}{\partial t}\right)_R+\left(\frac{\partial\langle E\rangle}{\partial t}\right)_{\rm ph}. \tag{4}$$

The first term on the right-hand side is due to carrier generation, the second is due to recombination, and the third is due to carrier-phonon interaction.

As mentioned above, we consider a homogeneously excited plasma. Thus we treat the carrier-density variation rate in a most simple way as contributed only by generation and recombination terms (however, in realistic experiments, diffusion also may be important),

$$\frac{dn}{dt}=G(t)+R. \tag{5}$$

The generation term in the energy rate equation [Eq. (4)] is due to the excess energy of the photoexcited e-h pair

$$\left(\frac{\partial\langle E\rangle}{\partial t}\right)_G=(E_L-\tilde{E}_g)G(t), \tag{6}$$

where E_L is the incident-photon energy and $\tilde{E}_g$ is the renormalized band gap. Assuming that the recombination results in disappearance of the average e-h pair energy, the term due to recombination in Eq. (4) is[26]

$$\left(\frac{\partial\langle E\rangle}{\partial t}\right)_R=\frac{\langle E\rangle}{n}R. \tag{7}$$

Inserting Eqs. (3) and (4) into the right-hand and left-hand sides of Eq. (2), respectively, yields the rate equation for the plasma effective temperature

$$\frac{dT}{dt}=\frac{\left(E_L-\tilde{E}_g-\frac{3}{2}k_BT\sum_i B^{1/2}_{-1/2}(\eta_i)\right)G(t)+\left[\frac{3}{2}k_BT\sum_i\left[B^{3/2}_{1/2}(\eta_i)-B^{1/2}_{-1/2}(\eta_i)\right]\right]R+\left(\frac{\partial\langle E\rangle}{\partial t}\right)_{\rm ph}}{\frac{3}{2}k_Bn\sum_i\left[\frac{5}{2}B^{3/2}_{1/2}(\eta_i)-\frac{3}{2}B^{1/2}_{-1/2}(\eta_i)\right]}. \tag{8}$$

Equation (8) generalizes the fermion heating effects both for photogeneration and recombination. For nondegenerate plasma, $B^{\alpha}_{\beta}(\eta_i)\equiv 1$, and the temperature rate equation simplifies to a convenient form

$$\frac{dT}{dt}=\frac{(E_L-\tilde{E}_g-3k_BT)G(t)+\left(\frac{\partial\langle E\rangle}{\partial t}\right)_{\rm ph}}{3k_Bn}. \tag{9}$$

Note that the recombination term in the numerator disappears.

The carrier photogeneration rate contained in Eq. (8) is determined by a laser pulse shape that is usually of Gaussian form with the full width at half magnitude τ_L,

$$G(t)=\frac{U_L}{\tau_L}\left(\frac{\beta}{\pi}\right)^{1/2}\exp\left(-\frac{\beta t^2}{\tau_L^2}\right), \tag{10}$$

where U_L is the total number of photons absorbed per unit volume, and $\beta=4\ln(2)$. The recombination is considered to originate from capture by deep centers and from direct band-to-band transitions,

$$R=-\frac{n}{\tau_c(T)}-R_{eh}(n,T). \tag{11}$$

We neglect the Auger recombination as there are no reasonable conditions for its manifestation in wide-gap semiconductors under consideration.[31] The rate of trapping by deep centers is assumed to be determined by MPE yielding an Arrhenius capture probability at room temperature and higher,[29]

$$\frac{1}{\tau_c(T)}=\frac{1}{\tau_c(T_0)}\left(\frac{T_0}{T}\right)^{3/2}\exp\left[\frac{W}{k_BT_0}\left(1-\frac{T_0}{T}\right)\right], \tag{12}$$

where T_0 is the equilibrium temperature and W is the height of the relevant localization barrier. Equation (12) implies that the quasitemperature of LO phonons, responsible for the capture, equals the carrier effective temperature, and the inverse radius of the deep traps is comparable with the dimension of the **k**-space region where the nonequilibrium LO phonons are excited.

The band-to-band recombination rate here is treated as due to spontaneous process and can be expressed through equilibrium-temperature bimolecular recombination coefficient $\gamma(T_0)$ referred to nondegenerate plasma,[32]

$$R_{eh}=\gamma(T_0)\left(\frac{T_0}{T}\right)^{3/2}\Xi_e(T)\Xi_h(T)\,\frac{2}{\sqrt{\pi}}\times\int_0^{\infty}\frac{\sqrt{x}\,dx}{\left\{\exp\left(\frac{\mu}{m_e}x-\eta_e\right)+1\right\}\left\{\exp\left(\frac{\mu}{m_h}x-\eta_h\right)+1\right\}}, \tag{13}$$

where m_i $(i=e,h)$ is the effective mass of electrons and holes and $\mu^{-1}=m_e^{-1}+m_h^{-1}$ is the inverse reduced one, $\Xi_i(T)=2(m_ik_BT/2\pi\hbar^2)^{3/2}$ is the effective density of states. For nondegenerate plasma,

$$R_{eh}=\gamma(T_0)\left(\frac{T_0}{T}\right)^{3/2}n^2. \tag{14}$$

The power due to carrier-phonon interaction is obtained by summing the rates of LO phonon production by carriers over all phonon modes **q**,

$$\left(\frac{\partial\langle E\rangle}{\partial t}\right)_{\rm ph}=-\frac{\hbar\omega_0}{V}\sum_{\mathbf{q}}\left(\frac{\partial\nu_{\mathbf{q}}}{\partial t}\right)_c=-\frac{\hbar\omega_0}{2\pi^2}\int_0^{q_M}\left(\frac{\partial\nu_q}{\partial t}\right)_c q^2dq, \tag{15}$$

where $\nu_{\mathbf{q}}$ is the average occupation number that in our spherically symmetric treatment is direction independent $(\nu_{\mathbf{q}}\equiv\nu_q)$. The rate of an LO phonon q generation by hot carriers via Fröhlich coupling with both phonon emission and absorption taken into account can be presented in the form similar to that in Ref. 33,

$$\left(\frac{\partial\nu_q}{\partial t}\right)_c=\frac{e^2(\kappa_\infty^{-1}-\kappa_0^{-1})\hbar\omega_0k_BT}{2\pi\varepsilon_0\hbar^5q^3(1+q_{\rm RPA}^2/q^2)^2}\left[\nu(T)-\nu_q\right]\times\sum_i m_i^2J_i\ln\left(1+\frac{f_i(E_{iq})}{\nu(T)}\right), \tag{16}$$

where κ_∞ and κ_0 are the optic and static permittivities, and J_i is the overlap integral[34] ($J_e=1$, $J_h\approx 0.5$). The threshold energy for the LO phonon emission is $E_{iq}=(2m_i\omega_0+\hbar c^2)^2/(8m_iq^2)$. Equation (16) includes screening of the carrier-phonon interaction within the model of static random-phase approximation (RPA) with the inverse squared screening length,

$$q_{\rm RPA}^2=\frac{ne^2}{\varepsilon_0\kappa_0k_BT}\sum_i B_{1/2}^{-1/2}(\eta_i). \tag{17}$$

The carrier-temperature LO phonon occupation number is

$$\nu(T)=\left[\exp\left(\frac{\hbar\omega_0}{k_BT}\right)-1\right]^{-1}. \tag{18}$$

To calculate the power transferred from plasma to LO phonons the occupation numbers are to be defined. The LO-phonon occupation number for each mode within the spherical **k**-space layer with the radius q can be calculated from the rate equation

$$\frac{d\nu_q}{dt}=\left(\frac{\partial\nu_q}{\partial t}\right)_c+\left(\frac{\partial\nu_q}{\partial t}\right)_{\rm nr}+\left(\frac{\partial\nu_q}{\partial t}\right)_N, \tag{19}$$

where the first term on the right-hand side is defined by Eq. (16), the second term is the phonon production rate due to nonradiative recombination by MPE process, and the third one is the rate of the anharmonic decay to daughter phonons.

The nonradiative recombination by MPE can result in accumulation of nonequilibrium phonons in the vicinity of the center of the Brillouin zone providing that the phonon emission probability depends on q as in the case of polar coupling. In strongly polar semiconductors, such as CdS and CdSe, the polar coupling dominates over the deformation potential coupling in Huang-Rhys factor when the radius of

the recombination center a_T exceeds a few lattice constants. Under such conditions the relevant LO phonon production rate is

$$\left(\frac{\partial \nu_q}{\partial t}\right)_{\rm nr} \approx \frac{n}{\tau_c}\frac{E_g}{\hbar\omega_0}\frac{2\pi^2}{q_T q^2(1+q_{\rm PRA}^2/q^2)^2}, \quad q \leqslant q_T, \tag{20}$$

where $q_T \cong \pi/a_T$. The condition $q_T \gg q_{\rm RPA}$ is to be fulfilled for strict holding of Eq. (20). The generation of long-wavelength nonequilibrium LO phonons by MPE process is negligible in GaAs-like crystals where the deformation-potential coupling dominates in the Huang-Rhys factor.[35]

The anharmonic term in Eq. (19) is assumed to be determined by a three-phonon process[21,22]

$$\left(\frac{\partial \nu_{\mathbf{q}}}{\partial t}\right)_N = -\frac{2\pi}{\hbar}\frac{2g^2}{V}\sum_{\mathbf{Q}}\frac{4\omega_{\mathbf{q}}\Omega_{\mathbf{Q}}\Omega_{\mathbf{q}-\mathbf{Q}}}{\omega_0^3} \times[\nu_{\mathbf{q}}(1+N_{\mathbf{Q}})(1+N_{\mathbf{q}-\mathbf{Q}})-N_{\mathbf{Q}}N_{\mathbf{q}-\mathbf{Q}}(1+\nu_{\mathbf{q}})] \times\delta(\hbar\omega_{\mathbf{q}}-\hbar\Omega_{\mathbf{Q}}-\hbar\Omega_{\mathbf{q}-\mathbf{Q}}), \tag{21}$$

where g is a certain constant,[36] $\Omega_{\mathbf{Q}}$ and $N_{\mathbf{Q}}$ are the frequency and the occupation number of the daughter phonons with the wave vector $\mathbf{Q}$. For dispersionless LO phonons ($\omega_{\mathbf{q}} \equiv \omega_0$) and linearly dispersed isotropic daughter phonons ($\Omega_{\mathbf{Q}} = \Omega_0 + cQ$) summing over angles can be performed yielding

$$\left(\frac{\partial \nu_q}{\partial t}\right)_N = -\frac{1}{\vartheta_0(0)Q_S^2 q} \times\int_{Q_S-\tilde{q}/2}^{Q_S+\tilde{q}/2}\frac{4\Omega_Q\Omega_{2Q_S-Q}}{\omega_0^2}Q(2Q_S-Q) \times[\nu_q(1+N_Q+N_{2Q_S-Q})-N_Q N_{2Q_S-Q}]dQ \quad \text{at } q \leqslant 2Q_S, \tag{22}$$

and

$$\left(\frac{\partial \nu_q}{\partial t}\right)_N = 0 \quad \text{at } q > 2Q_S, \tag{23}$$

where Q_S is the daughter-phonon wave number at the subharmonic frequency $\Omega_{Q_S} = \omega_0/2$; the width of the integration interval is

$$\tilde{q} = \min[q, 2(q_M - Q_S)]. \tag{24}$$

The zero-temperature zone-center lifetime $\vartheta_0(0)$, employed in Eq. (22), is a function of the anharmonic constant g and daughter-phonon group velocity c.[22] Note that Eq. (23) introduces ''nondecaying'' short-wavelength LO phonons, which are possible only for a nonsphalerite lattice vibration spectrum where the ''subharmonic'' wave number may by smaller than $q_M/2$ (see Fig. 1). Here, the inability to decay refers to the tree-phonon process under consideration, so that other routes of anharmonic relaxation may be possible but are assumed to be of insignificant efficiency.

Under convenient assumption that the decay products of the nonequilibrium LO phonons are rapidly scattered all over the Brillouin zone and no second nonequilibrium-phonon bottleneck occurs, Eq. (22) reduces, and, for zone-center LO phonons decaying via three-phonon process,

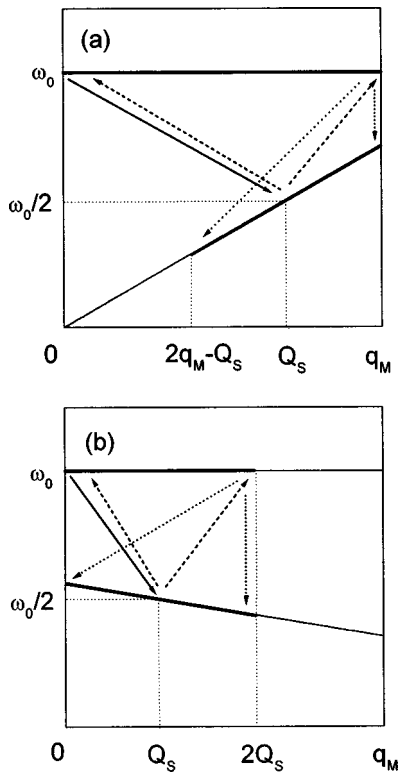

FIG. 1. Interplay of nonequilibrium phonons of two generations for simplified lattice vibration spectra in type-I (a) and type-II (b) crystals. Bold sections, modes coupled via three-phonon interbranch interaction; fine sections, ''nondecaying'' LO phonons and ''nonfusing'' daughter-branch phonons. Solid arrows, decay of long-wavelength LO phonons to subharmonic phonons; dashed arrows, fusion of subharmonic phonons to a wide spectrum of LO phonons; dotted arrows, decay of short-wavelength LO phonons to a wide spectrum of daughter phonons.

$$\left(\frac{\partial \nu_0}{\partial t}\right)_N = -\frac{\nu_0(N_{Q_S}^{(0)}+1)^2-(N_{Q_S}^{(0)})^2(\nu_0+1)}{\vartheta_0(0)} \equiv -\frac{\nu_0-\nu_0^{(0)}}{\vartheta_0(T_0)}, \tag{25}$$

where $\nu_0^{(0)}$ and $N_{Q_S}^{(0)}$ are the equilibrium occupation numbers of the LO phonons and of the subharmonic phonons, respectively, and $\vartheta_0(T_0)$ is the LO-phonon depopulation time at the ambient temperature.[22]

The second-generation (daughter) nonequilibrium phonons are the products of the anharmonic decay of the LO phonons referred to as nonequilibrium phonons of the first generation. The daughter nonequilibrium phonons may accumulate in the lower-frequency vibration modes and fuse back to the LO phonons, thus reducing the total rate of the relaxation. Assuming that the higher-generation phonons are almost in equilibrium, the occupation numbers of the daughter phonons obey the rate equation

$$\frac{dN_Q}{dt} = \left(\frac{\partial N_Q}{\partial t}\right)_\nu - \frac{N_Q - N_Q^{(0)}}{\Theta_Q(T_0)}, \tag{26}$$

where the first term on the right-hand side is the rate of the daughter phonon production by LO phonons and the second term is the rate of the anharmonic relaxation via decay to a wide spectrum of lower-frequency phonons. $\Theta_Q(T_0)$ is the characteristic time constant of the relaxation at the ambient temperature. The daughter phonons are produced via the three-phonon process with a rate[22]

$$\left(\frac{\partial N_{\mathbf{Q}}}{\partial t}\right)_{\nu} = -\frac{2\pi}{\hbar}\frac{4g^2}{V}\sum_{\mathbf{q}}\frac{4\omega_{\mathbf{q}}\Omega_{\mathbf{Q}}\Omega_{\mathbf{q}\text{-}\mathbf{Q}}}{\omega_0^3} \times[N_{\mathbf{Q}}N_{\mathbf{q}\text{-}\mathbf{Q}}(1+\nu_{\mathbf{q}})-\nu_{\mathbf{q}}(1+N_{\mathbf{Q}})(1+N_{\mathbf{q}\text{-}\mathbf{Q}})] \times\delta(\hbar\omega_{\mathbf{q}}-\hbar\Omega_{\mathbf{Q}}-\hbar\Omega_{\mathbf{q}\text{-}\mathbf{Q}}). \quad (27)$$

Again, for dispersionless LO phonons and linearly dispersed daughter phonons summing over angles under isotropic condition yields

$$\left(\frac{\partial N_Q}{\partial t}\right)_{\nu} = -\frac{2(2Q_S-Q)}{\vartheta_0(0)Q_S^2Q}\times\int_{2|Q_S-Q|}^{\tilde{Q}}\frac{4\Omega_Q\Omega_{2Q_S-Q}}{\omega_0^2} \times q[N_QN_{2Q_S-Q}-\nu_q(1+N_Q+N_{2Q_S-Q})]dq \quad \text{at } 2Q_S-q_M\leqslant Q\leqslant 2Q_S \quad (28)$$

and

$$\left(\frac{\partial N_Q}{\partial t}\right)_{\nu}=0 \quad \text{at } Q>2Q_S \quad \text{and } Q<2Q_S-q_M. \quad (29)$$

The upper limit of the integration in Eq. (28) is

$$\tilde{Q}=\min(q_M,2Q_S). \quad (30)$$

Now Eq. (29) introduces ''nonfusing'' daughter-branch phonons with the same reservations as for ''nondecaying'' LO phonons.

Equations (21)–(24) and (26)–(30) describe a complex interplay between nonequilibrium phonons of two generations for the simplified lattice vibration spectra. This interplay is schematically depicted in Fig. 1 for two types of the spectrum with different values of the relative subharmonic wave number Q_S/q_M. The sections of the phonon branches containing modes capable for interbranch interaction (fission of LO modes to daughter modes and fusion of daughter modes back to LO modes) are depicted as bold. Fine lines represent modes for which restrictions for interbranch interactions occur as described by Eqs. (23) and (29). The value of Q_S/q_M is seen to be the key factor for the occurrence of the second-nonequilibrium-phonon bottleneck.

First, we consider a GaAs-type crystal [Fig. 1(a)] with the condition $Q_S>q_M/2$ held. Here, an LO phonon from any mode can decay into two phonons of the subharmonic branch according to Eq. (22), as well as any LO mode can be filled by a phonon fused of two appropriate daughter phonons. However, the interbranch energy transfer does not involve the zone-center part of the daughter branch. The ''nonfusing'' daughter-branch phonons here are determined by the condition $Q<2Q_S-q_M$. The inability of these phonons to fuse to LO phonons originates from the absence of a pair-daughter phonon satisfying the energy conservation. However, the ''nonfusing'' region contains a small amount of phonon modes except for cases when the subharmonic wave number is very close to the zone boundary. Thus, the crucial peculiarity of the GaAs-type lattice dynamics is an involvement of a large amount of short-wavelength phonons from both branches into the energy transfer. As it was pointed out in Ref. 21, this results in rapid fusion of the second-generation nonequilibrium phonons, initially produced in a narrow segment of width $\tilde{q}$ [see Eq. (24)], into zone-edge LO phonons that are difficult to bring out of equilibrium because of a large amount of modes. A more realistic shape of the LO branch may reduce the influence of the short-wavelength LO phonons to some extent;[22] however, the principle features of the relaxation remain only slightly changed. We designate the above described anharmonic interbranch relaxation with zone boundary phonons involved as type-I second nonequilibrium-phonon bottleneck.

With decreasing Q_S, the number of ''nonfusing'' daughter modes reduces, and at $Q_S=q_M/2$ the whole daughter branch is exploited. However, a subsequent reduction of the subharmonic wave number invokes dramatic changes in the energy transfer. Figure 1(b) presents a case for lattice dynamics with $Q_S<q_M/2$. Now, ''nonfusing'' daughter modes appear in the short-wavelength region above $2Q_S$. Additionally, LO modes in the same large-wave-number region lose the ability to decay through the three-phonon process under consideration. The ''nondecaying'' LO modes also cannot be filled by fusing a pair of daughter phonons. The number of phonon modes participating in the relaxation process thus can be considerably reduced, e.g., in a crystal with $Q_S\approx 0.3q_M$, about 80% of the modes in both branches are eliminated from the interplay. A small number of the daughter phonon modes can be easily filled by decay of the LO phonons and thus substantially hinder the relaxation. We designate this kind of anharmonic interbranch relaxation with zone boundary phonons excluded from the interplay as type-II second nonequilibrium-phonon bottleneck.

III. CALCULATIONS AND DISCUSSION

The material-parameter set used in the calculations was that of CdS used in Ref. 20 except for phonon depopulation time constants. Zero-temperature LO-phonon lifetime (2.1 ps) was deduced from a precise value of the Raman linewidth.[37] Following the ''ω^{-5}'' rule,[36] the subharmonic-phonon lifetime of 67 ps at $T_0=0$ was estimated. The room-temperature depopulation time of daughter phonons (12.4 ps) was obtained under assumption of their further decay to pairs of phonons around the frequency $\omega_0/4$ as

$$\Theta(T_0)=\Theta(0)\left[1+2\Big/\left\{\exp\left(\frac{\hbar\omega_0}{4k_BT_0}\right)-1\right\}\right]^{-1}. \quad (31)$$

The laser-pulse parameters used were $E_L=3.50$ eV and $\tau_L=28$ ps. Experimental values of the carrier lifetime (760 ps) and localization barrier height (110 meV) were used.[29] The radius of the dominating recombination center was equated with one lattice constant to avoid overestimation of the nonradiative MPE process.

A. Carrier density

We start presenting the results from carrier effective-temperature evolution calculated for the whole model de-

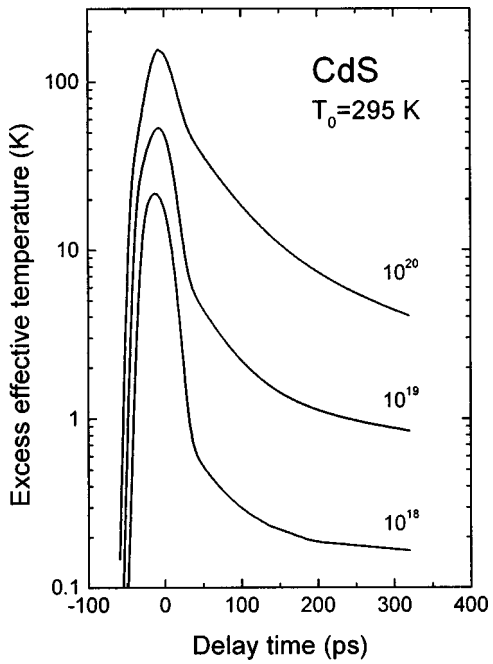

FIG. 2. Evolution of the carrier effective temperature with time in a CdS crystal, excited by a 28-ps laser pulse, for different total numbers of photons absorbed per cm^3.

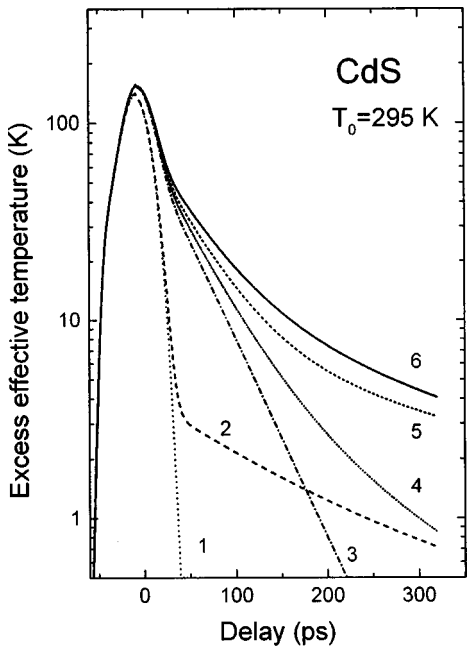

FIG. 3. Kinetics of carrier cooling in a CdS crystal, excited by 10^{20} photons/cm^3, for different models employed: ''bare'' first nonequilibrium-phonon bottleneck (1), recombination heating without second nonequilibrium-phonon bottleneck (2), ''bare'' second bottleneck (3), second bottleneck with fermion recombination heating (4), the same with LO phonon production via carrier capture by MPE (5), all mechanisms taken into account (6).

scribed in Sec. II. Although the lattice vibration spectra of CdS is anisotropic, we employed an average value of the subharmonic wave number $Q_S \approx 0.3 q_M$, based on estimations presented in Ref. 20, to model conditions for type-II second nonequilibrium-phonon bottleneck. Figure 2 depicts kinetics obtained for three values of the total number of photons absorbed per unit volume (for carrier lifetime much larger than the laser-pulse duration this number only slightly exceeds the peak-carrier density). One can see that a slow component of the relaxation always exist. However, for $U_L < 10^{19}$ cm^{-3} the effect is negligible and is unlikely to be noticed in an experiment performed with a convenient accuracy. Above 10^{19} cm^{-3}, the slow component emerges to a noticeable extent, and the plasma cooling is to be considered as not terminated within the first 100 ps, at least.

B. Slow-relaxation factors

The model used for calculating the kinetics presented in Fig. 2 conceals a few mechanisms accounting for slow cooling. To elucidate the role of each mechanism a calculation with sequential switch-on of various factors was performed at $U_L = 10^{20}$ cm^{-3} (Fig. 3). Curve 1 depicts the variation of the carrier effective temperature with time for a ''bare'' first nonequilibrium-phonon bottleneck: both recombination heating mechanisms—fermion recombination and nonradiative recombination—are excluded and the second bottleneck is ignored $[\Theta(T_0) = 0]$. The excess effective temperature is seen to vary concurrently with the excitation, as the room-temperature LO-phonon depopulation time in CdS ($\approx$0.5 ps) is much smaller than the laser-pulse duration utilized in the calculation.

Next, curve 2 is the case when the recombination heating (both mechanisms) is taken into account. A slow-relaxation component is seen to emerge with the decay time constant comparable with the carrier lifetime. However, at room temperature, the magnitude of the temperature increase due to recombination heating is far too small to be important (this may not be held for cryogenic ambient temperatures[27]). Again, curve 3 shows the relaxation for a ''bare'' second bottleneck without recombination heating taken into account. The excess effective temperature now is seen to maintain a noticeable value just after termination of the excitation pulse and to subsequently relax almost exponentially. The striking feature of the relaxation is that the relaxation time constant ($\tau = 42$ ps) considerably exceeds the depopulation time of the daughter phonons $\Theta(T_0) = 12.4$ ps (this effect is discussed in detail below in Sec. III C).

Comparison of the latter two curves with that obtained with both the recombination heating and the second bottleneck being taken into account (curve 6) infers that the cooling rate is generally determined by the recombination rate of long-living nonequilibrium carriers. Meanwhile, the magnitude of the excess temperature at large delay is substantially increased because of the second nonequilibrium-phonon bottleneck. Eventually, it is obvious that for carrier densities above 10^{19} cm^{-3} a combined action of the second nonequilibrium-phonon bottleneck and recombination heating results in a noticeable slow component of the plasma cooling on a time scale of hundreds of picoseconds.

The relative contribution of each recombination-heating mechanism can be estimated from curves 4 and 5 in Fig. 3. The effect of the second bottleneck combined with only the fermion recombination heating is depicted by curve 4; the same but with only the heating due to production of nonequilibrium LO phonons in the MPE process is depicted by curve 5. The relative contribution of each recombination heating

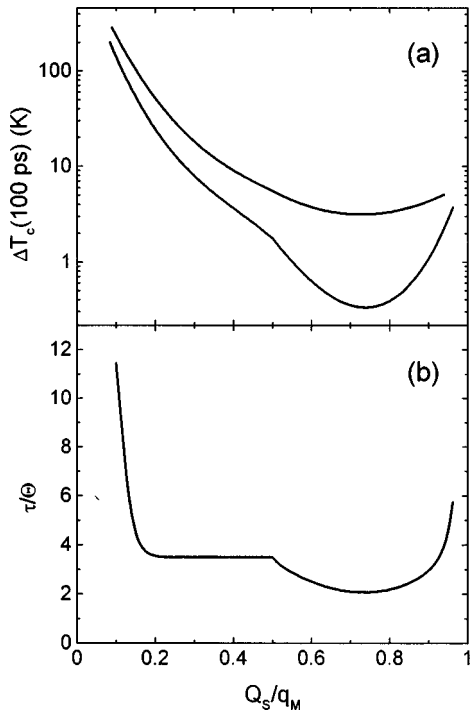

FIG. 4. (a) Residual excess effective temperature after 100-ps delay in a CdS crystal, excited by 10^{20} photons/cm^3, as a function of the relative subharmonic wave number. Lower curve, ''bare'' second bottleneck; upper curve, the same with the recombination heating taken into account. (b) Slow-relaxation time constant (in daughter-phonon depopulation-time units) vs subharmonic wave number.

mechanism is seen to be of the same order, though it may vary in real situations depending on carrier lifetime, degree of degeneracy, dimensions of deep centers, etc.

C. ''Bare'' second bottleneck

It is worth discussing the second bottleneck in more detail under conditions of the absence of the recombination heating, as the relevant effective-temperature relaxation time significantly exceeds the daughter-phonon depopulation time as discussed above. Our analysis shows that this effect is determined by the relative location of the subharmonic wave number, i.e., by the ratio Q_S/q_M. A set of cooling curves for different values of the subharmonic wave number was calculated. The results for $U_L=10^{20}$ cm^{-3} are generalized in Fig. 4. Figure 4(a) depicts variation of the excess carrier temperature at a 100-ps delay with Q_S (lower and upper curves represent the bottleneck in the ''bare'' form and with the recombination heating taken into account, respectively). The residual excess temperature is seen to increase when the subharmonic wave number approaches either the zone boundary (type-I second bottleneck) or the zone center (type-II), the latter effect being more pronounced. This is easily understood as in both cases the number of the daughter modes involved into energy transfer is substantially reduced, and the second bottleneck ''narrows'' (see Fig. 1). However, the most striking feature of the relaxation is that the time constant for the ''bare'' bottleneck always exceeds the second-generation phonon lifetime Θ as shown in Fig. 4(b). For the most unfavorable conditions ($Q_S\approx 0.7$) the ratio τ/Θ does not drop below the value of 2. Our simulations have shown that this ratio does not depend on the excited carrier density and thus is determined only by lattice vibration spectra. The effect can be understood in terms of a simplified approach to the interplay of two phonon branches as presented below.

Consider an LO and a daughter branch with the number of modes effectively involved into interaction λ and Λ, which are uniformly occupied with average numbers $\overline{\nu}$ and $\overline{N}$, respectively. At the relaxation stage, the temporal evolution of the occupation numbers can be described by a system of equations,[20]

$$\frac{d\overline{\nu}}{dt}=-\frac{\overline{\nu}(\overline{N}+1)^2-\overline{N}^2(\overline{\nu}+1)}{\vartheta(0)},$$
$$\frac{d\overline{N}}{dt}=\frac{2\lambda}{\Lambda}\frac{\overline{\nu}(\overline{N}+1)^2-\overline{N}^2(\overline{\nu}+1)}{\vartheta(0)}-\frac{\overline{N}-\overline{N}^{(0)}}{\Theta(T_0)}. \tag{32}$$

For small excess occupations $\Delta\overline{\nu}=\overline{\nu}-\overline{\nu}^{(0)}$ and $\Delta\overline{N}=\overline{N}-\overline{N}^{(0)}$, the condition $\Theta\gg\vartheta(0)$ being held, the solution of the system is

$$\Delta\overline{\nu},\Delta\overline{N}\propto\exp(-t/\tau), \tag{33}$$

where the relaxation time constant is

$$\tau=\Theta(T_0)\left[1+\frac{\lambda}{\Lambda}\frac{4(\overline{N}^{(0)}-\overline{\nu}^{(0)})}{2\overline{N}^{(0)}+1}\right]$$
$$\approx\begin{cases}\Theta(T_0) & \text{at low temperature } (\overline{N}^{(0)}\ll 1)\\ \Theta(T_0)(1+\lambda/\Lambda) & \text{at high temperature } (\overline{N}^{(0)}>1).\end{cases} \tag{34}$$

In the high-temperature limit, the relaxation time enhances because of the nonzero equilibrium occupation of subharmonic phonons, probably, because of fusion of nonequilibrium daughter phonons with equilibrium ones. The magnitude of the enhancement is related with the ratio λ/Λ that substitutes an actual complex distribution of nonequilibrium phonons within two branches. For the subharmonic wave number close to half of the zone dimension, both branches are heated almost entirely ($\lambda/\Lambda\approx 1$), and Eq. (34) yields $\tau\approx 2\Theta$, which is in line with the results presented in Fig. 4(b). For a well-pronounced type-I second bottleneck the relaxation time increases due to the exclusion of long-wavelength daughter modes [see Fig. 1(a)]. Meanwhile, for a type-II bottleneck, short-wavelength daughter modes are excluded, but some nondecaying LO modes still indirectly participate in the relaxation as they are coupled with the carrier system. This is identical to a growth of the ratio λ/Λ and, consequently, in a steep increase of the relaxation time constant for small values of Q_S as shown in Fig. 4(b).

IV. CONCLUSIONS

A revision of the second-generation nonequilibrium phonon bottleneck model was performed. We have shown that, in combination with relatively inefficient recombination heating processes (fermion recombination heating and generation of nonequilibrium LO phonons due to nonradiative capture via MPE), the second bottleneck manifests itself by

slowing the plasma cooling even at room temperature. For photogenerated carrier densities above 10^{19} cm^{-3} an instrumentally distinguishable slow-cooling phase emerges with the relaxation time constant $\sim$100 ps, determined by carrier lifetime, and with the residual excess temperature determined by daughter-phonon depopulation time. However, the most striking result obtained here is that, even with the recombination heating being negligible, the relevant effective-temperature relaxation time constant exceeds the daughter-phonon depopulation time for at least 2–3 times due to complex interplay between both nonequilibrium and equilibrium phonons of two branches. The efficiency of the second bottleneck was shown to be strongly dependent on lattice vibration spectrum, and the most favorable conditions for its manifestation are realized in crystals with the wave number of the subharmonic phonon less than half of the zone radius (type-II bottleneck).

The calculations presented above are in qualitative agreement with former experimental results.[11–18] However, for quantitative fitting, factors determining the carrier density are to be treated in detail, according to experimental conditions.

The sensitivity of the manifestation of the ''slow'' phase in carrier cooling to recombination processes and lattice vibration spectrum may be the cause of ambiguous data on carrier cooling rate in low-dimensional semiconductor structures.[38] Different density of phonon modes, confinement effects, and ''folding'' of phonon branches may originate a variety of second-bottleneck configurations here. Meanwhile the centers of nonradiative recombination, especially those related with interfaces, may result in unpredictable role of recombination heating.

ACKNOWLEDGMENT

The work was supported by the Lithuanian State Science and Studies Foundation.

*Electronic address: arturas.zukauskas@ff.vu.lt

[1] R. F. Leheny, J. Shah, R. L. Fork, C. V. Shank, and A. Migus, Solid State Commun. **31**, 809 (1979).
[2] D. von der Linde and R. Lambrich, Phys. Rev. Lett. **42**, 1090 (1979).
[3] S. Tanaka, H. Kobayashi, H. Saito, and S. Shionoya, J. Phys. Soc. Jpn. **49**, 1051 (1980).
[4] W. Graudszus and E. O. Göbel, Physica B **117/118**, 555 (1983).
[5] H. M. van Driel, Phys. Rev. B **19**, 5928 (1979).
[6] W. Pötz and P. Kocevar, Phys. Rev. B **28**, 7040 (1983).
[7] U. Hohenester, P. Supancic, P. Kocevar, X. Q. Zhou, W. Kütt, and H. Kurtz, Phys. Rev. B **47**, 13 233 (1993).
[8] S. S. Prabhu, A. S. Vengurlekar, S. K. Roy, and J. Shah, Phys. Rev. B **51**, 14 233 (1995).
[9] A. C. S. Algarte, A. R. Vasconcellos, and R. Luzzi, Phys. Rev. B **54**, 11 311 (1996).
[10] S. E. Kumekov and V. I. Perel, Zh. Eksp. Teor. Fiz. **94**, 346 (1988) [Sov. Phys. JETP **67**, 193 (1988)].
[11] R. J. Seymour, M. R. Junnarkar, and R. R. Alfano, Solid State Commun. **41**, 657 (1982).
[12] S. S. Yao and R. R. Alfano, Phys. Rev. B **26**, 4781 (1982).
[13] T. Amand and J. Collet, J. Phys. Chem. Solids **46**, 1053 (1985).
[14] M. R. Junnarkar and R. R. Alfano, Phys. Rev. B **34**, 7045 (1986).
[15] R. Baltramiejūnas, A. Žukauskas, V. Latinis, V. Stepankevičius, and S. Juršėnas, Fiz. Tekh. Poluprovodn. **21**, 932 (1987) [Sov. Phys. Semicond. **21**, 568 (1987)].
[16] R. Baltramiejūnas, A. Žukauskas, V. Latinis, and S. Juršėnas, Pis'ma Zh. Eksp. Teor. Fiz. **46**, 67 (1987) [JETP Lett. **46**, 80 (1987)].
[17] R. Baltramiejūnas and A. Žukauskas, Phys. Status Solidi B **149**, 337 (1988).
[18] R. Baltramiejūnas, S. Juršėnas, A. Žukauskas, and E. Kuokštis, Fiz. Tverd. Tela (Leningrad) **31**, 259 (1989) [Sov. Phys. Solid State **31**, 1984 (1989)].
[19] S. Juršėnas, A. Žukauskas, and R. Baltramiejūnas, J. Phys.: Condens. Matter **4**, 9987 (1992).
[20] A. Žukauskas and S. Juršėnas, Phys. Rev. B **51**, 4836 (1995).
[21] K. Král and B. Hejda, Phys. Status Solidi B **174**, 209 (1992).
[22] B. Hejda and K. Král, Phys. Rev. B **47**, 15 554 (1993).
[23] V. Klimov, P. Haring Bolivar, and H. Kurz, Phys. Rev. B **52**, 4728 (1995).
[24] P. Langot, N. Del Fatti, D. Christofilos, R. Tommasi, and F. Vallée, Phys. Rev. B **54**, 14 487 (1996).
[25] K. T. Tsen, R. P. Joshi, D. K. Ferry, A. Botchkarev, B. Sverdlov, A. Salvador, and H. Morkoç, Appl. Phys. Lett. **68**, 2990 (1996).
[26] D. Bimberg and J. Mycielski, Phys. Rev. B **31**, 5490 (1985).
[27] K. Leo and W. W. Rühle, Solid State Commun. **62**, 659 (1987).
[28] C. H. Henry and D. V. Lang, Phys. Rev. B **15**, 989 (1977).
[29] S. Juršėnas, G. Kurilčik, and A. Žukauskas, Phys. Rev. B **54**, 16 706 (1996).
[30] U. Wenschuh, E. Heiner, and P. Fulde, Phys. Status Solidi B **173**, 221 (1992).
[31] A. Haug, J. Phys. C **16**, 4159 (1983).
[32] Y. P. Varshni, Phys. Status Solidi **19**, 459 (1967).
[33] Sh. M. Kogan, Fiz. Tverd. Tela (Leningrad) **4**, 2474 (1962) [Sov. Phys. Solid State **4**, 1813 (1963)].
[34] J. D. Wiley, Phys. Rev. B **4**, 2485 (1971).
[35] B. K. Ridley, *Quantum Processes in Semiconductors* (Clarendon, Oxford, 1982), Chap. 6.
[36] P. G. Klemens, Phys. Rev. **148**, 845 (1966).
[37] T. C. Damen, R. C. C. Leite, and J. Shah, in *Proceedings of the Tenth International Conference on the Physics of Semiconductors*, edited by S. P. Keller, J. C. Hensel, and F. Stern (U.S. Atomic Energy Commission, Oak Ridge, 1970), p. 735.
[38] Y. Rosenwaks, M. C. Hanna, D. H. Levi, D. M. Szmyd, R. K. Ahrenkiel, and A. J. Nozik, Phys. Rev. B **48**, 14 675 (1993).